The Reactions of Selected Acetates with the OH Radical in the Presence of NO: Novel Rearrangement of Alkoxy Radicals of Structure RC(O)OCH(Ȯ)Ŕ

Ernesto C. Tuazon,[†] Sara M. Aschmann,[†] Roger Atkinson,[†,§] and William P. L. Carter*[,†,‡]

Statewide Air Pollution Research Center and College of Engineering, Center for Environmental Research & Technology, University of California, Riverside, California 92521

Received: November 5, 1997; In Final Form: January 20, 1998

Products of the gas-phase reactions of the OH radical with ethyl acetate, isopropyl acetate, *tert*-butyl acetate in the presence of NO were investigated using *in situ* Fourier transform infrared spectroscopy and gas chromatography. The products identified and their molar formation yields (corrected for secondary reactions with the OH radical) were acetic acid (0.96 ± 0.08) from ethyl acetate; acetic acid (0.09 ± 0.03), acetic anhydride (0.76 ± 0.07), and acetone (0.24 ± 0.02) from isopropyl acetate; and acetic anhydride (0.49 ± 0.05) and acetone (0.20 ± 0.02) from *tert*-butyl acetate. Consideration of the potential reaction pathways of the intermediate alkoxy radicals leads to the conclusion that alkoxy radicals of structure RC(O)OCH(Ȯ)Ŕ can undergo a rapid rearrangement and decomposition (α-ester rearrangement) to RC(O)OH plus ŔĊO, presumably via a five-membered ring transition state. However, our product studies provided no evidence for the analogous *β*-ester rearrangement proceeding via a six-membered transition state, although the possibility that this reaction could occur is not ruled out.

Introduction

The tropospheric degradations of volatile organic compounds emitted into the atmosphere from anthropogenic and biogenic sources generally involve the intermediate formation of organic peroxy ($R\dot{O}_2$) and alkoxy ($R\dot{O}$) radicals.[1,2] The tropospheric degradations of most volatile organic compounds not containing >C═C< bonds (for example, alkanes, haloalkanes, ethers, carbonyls, and esters) are initiated by reaction with the OH radical to form an alkyl or substituted alkyl ($\dot{R}$) radical, which then rapidly adds O_2 to form an organic peroxy ($R\dot{O}_2$) radical.[1,2] In the presence of NO, peroxy radicals react with NO to form the corresponding alkoxy radical plus NO_2, together with formation of an organic nitrate from the larger ($\geq C_3$) organic peroxy radicals.[1,2]

$$OH + RH \longrightarrow H_2O + \dot{R} \quad (1)$$

$$\dot{R} + O_2 \xrightarrow{M} R\dot{O}_2 \quad (2)$$

$$R\dot{O}_2 + NO \longrightarrow \dot{R}O + NO_2 \quad (3a)$$

$$R\dot{O}_2 + NO \xrightarrow{M} RONO_2 \quad (3b)$$

Alkoxy radicals are important intermediates in organic photooxidations because they can undergo a number of competing reactions, resulting in much of the complexity and uncertainty in the atmospheric chemistry of organic compounds.

On the basis of studies of alkoxy and *β*-hydroxyalkoxy radicals formed from the OH radical-initiated reactions of alkanes and alkenes, respectively, the important reactions of alkoxy radicals under tropospheric conditions are recognized to be reaction with O_2, decomposition by C−C bond scission, and a 1,5-H shift isomerization through a six-membered transition state.[2,3] These reactions are shown in Scheme 1 for the 2-pentoxy radical formed in the OH radical-initiated reaction of *n*-pentane in the presence of NO.

SCHEME 1

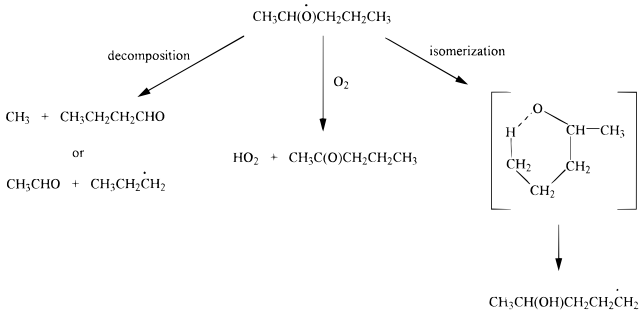

Analogous reactions of alkoxy radicals formed from other classes of organic compounds, including ketones and ethers, are observed,[1,4] and it has been assumed that all alkoxy radicals react in the troposphere by decomposition, 1,5-H shift isomerization through a six-membered transition state involving abstraction of an H-atom by the alkoxy oxygen atom, and reaction with O_2.

However, these known reactions of alkoxy radicals could not explain the results of environmental chamber experiments when ethyl acetate was added to irradiated NO_x−organic−air mixtures.[5] Computer modeling of these experiments could not simulate the unexpectedly high peroxyacetyl nitrate (PAN, $CH_3C(O)OONO_2$) yields nor the O_3 and NO_2 time−concentration profiles unless it was assumed that the ethyl acetate photooxidation mechanism was dominated by pathways forming acetyl ($CH_3\dot{C}O$) or acetyl peroxy ($CH_3C(O)O\dot{O}$) radicals, the precursors of PAN. It was initially thought that PAN formation

* To whom correspondence should be addressed.
† Statewide Air Pollution Research Center.
‡ College of Engineering.
§ Also Department of Environmental Science and Department of Chemistry, University of California, Riverside, California 92521.

S1089-5639(98)00081-4 CCC: $15.00
Published on Web 03/26/1998

may be due to direct formation of acetyl radicals from the reaction

$$CH_3C(O)OCH(O\dot{O})CH_3 \rightarrow CH_3C(O)O\dot{O} + CH_3CHO \quad (4)$$

which would involve an O-atom transfer via a six-membered ring transition state. However, the high yield of acetaldehyde predicted by this reaction was not observed.[5] The other alternative is the formation of acetyl radicals from the corresponding alkoxy radical, by the reaction,

$$CH_3C(O)OCH(\dot{O})CH_3 \rightarrow CH_3C(O)OH + CH_3\dot{C}O \quad (5)$$

which involves an H-atom transfer through a five-membered ring transition state. While the occurrence of reaction 5 could explain the experimental data obtained,[5] acetic acid was not monitored in the NO_x−organic−ethyl acetate−air irradiations. To obtain more definitive evidence concerning this possible reaction 5, we have carried out product studies of the gas-phase reactions of the OH radical with ethyl acetate [$CH_3C(O)OCH_2CH_3$], isopropyl acetate [$CH_3C(O)OCH(CH_3)_2$], and *tert*-butyl acetate [$CH_3C(O)OC(CH_3)_3$] in the presence of NO.

Experimental Section

Experiments were carried out in a 5800 L evacuable, Teflon-coated chamber containing a multiple reflection optical system interfaced to a Nicolet 7199 Fourier transform infrared (FT-IR) absorption spectrometer and with irradiation provided by a 24-kW xenon arc filtered through a 0.25 in. thick Pyrex pane (to remove wavelengths <300 nm). Hydroxyl radicals were generated in the presence of NO by the photolysis of methyl nitrite (CH_3ONO) in air at wavelengths >300 nm,[6]

$$CH_3ONO + h\nu \rightarrow CH_3\dot{O} + NO \quad (6)$$

$$CH_3\dot{O} + O_2 \rightarrow HCHO + HO_2 \quad (7)$$

$$HO_2 + NO \rightarrow OH + NO_2 \quad (8)$$

and NO was added to the reactant mixtures to suppress the formation of O_3 and hence of NO_3 radicals.[6]

The initial concentrations of the esters, CH_3ONO, and NO were (1.23−2.46) × 10^{14} molecule cm^{-3}, 2.46 × 10^{14} molecule cm^{-3}, and (0.74−1.47) × 10^{14} molecule cm^{-3}, respectively. Vapors of the reactants were measured into calibrated 2 and 5 L Pyrex bulbs with an MKS Baratron 0−100 Torr sensor and flushed into the 5800 L chamber containing air (a synthetic mixture of 80% N_2 and 20% O_2) at 298 ± 2 K and 740 Torr total pressure. The majority of the experiments were conducted with continuous irradiation (20−65 min duration) and were monitored by FT-IR spectroscopy with 64 coadded interferograms (scans) per spectrum (1.8 min measurement time) recorded with a full-width-at-half-maximum (fwhm) resolution of 0.7 cm^{-1} and a path length of 62.9 m. Experiments which employed intermittent irrradiation (with illumination periods of 10−16 min) were also carrried out, with both FT-IR and gas chromatographic analyses being performed during the intervening dark periods.

Quantitative reference spectra of acetic acid were obtained with weighed amounts of the liquid sample which were vaporized into the chamber, thus avoiding errors in partial pressure measurements due to dimer formation in the vapor phase at Torr concentrations. [The base line-referenced absorptivity of the P-branch peak of $CH_3C(O)OH$ at 1781.4 cm^{-1} (Q-branch at 1790.3 cm^{-1}) was measured to be (4.44 ± 0.18) × 10^{-19} $molecule^{-1}$ cm^2]. A similar calibration was employed for acetic anhydride and agreed with the method of partial pressure measurements described above for the reactants. Reference infrared spectra for other products were available from previous calibrations in this laboratory.[7]

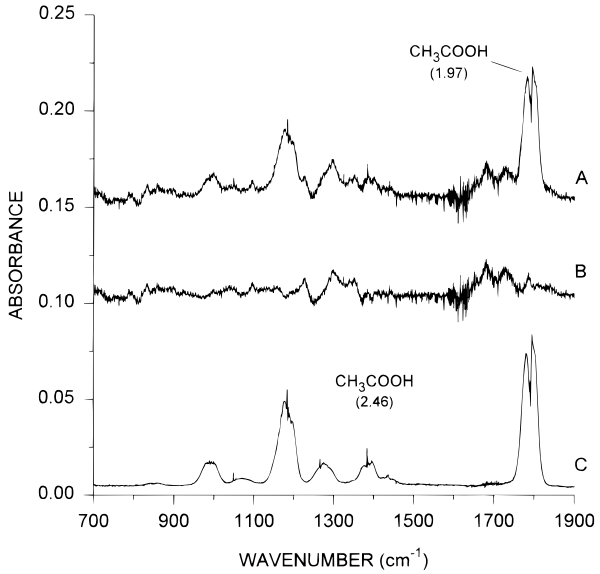

Figure 1. Infrared spectra from a CH_3ONO−NO−ethyl acetate−air irradiation. (A) Products attributed to reaction of ethyl acetate; photolysis time = 61 min; ethyl acetate reacted = 2.12 × 10^{13} molecule cm^{-3}. (B) Residual product spectrum. (C) Reference spectrum of gaseous acetic acid (monomeric form). The numbers in parentheses are concentrations in units of 10^{13} molecule cm^{-3}.

For selected experiments with isopropyl acetate and *tert*-butyl acetate, 100 cm^3 volume gas samples were collected onto Tenax-TA solid adsorbent for subsequent thermal desorption and analysis (primarily of acetone and acetaldehyde) by gas chromatography with flame ionization detection (GC−FID). The gas samples collected on the Tenax solid adsorbent were thermally desorbed at ∼225 °C onto a 30 m DB-1701 megabore column held at −40 °C, which was then temperature programmed to 200 °C at 8 °C min^{-1}. GC−FID response factors for acetone and acetaldehyde were determined by introducing measured amounts of these carbonyls into a reaction chamber and conducting replicate GC−FID analyses, as described previously.[8]

The chemicals used, as well as their stated purities, were acetic acid (99.7%) and acetone (HPLC Grade), Fisher Scientific; acetaldehyde (99.5+%), acetic anhydride [$CH_3C(O)OC(O)CH_3$] (99+%), *tert*-butyl acetate (99+%), ethyl acetate (99.8%), and isopropyl acetate (99%), Aldrich Chemical Co.; and NO (≥99.0%), Matheson Gas Products. Methyl nitrite was prepared as described by Taylor et al.[9] and stored under vacuum at 77 K.

Results

A series of CH_3ONO−NO−acetate−air irradiations were carried out, with analyses of reactants and products by FT-IR absorption spectroscopy and GC−FID. Figure 1 shows the FT-IR spectroscopic detection of acetic acid as the main product observed from ethyl acetate, with Figure 1A being obtained from the spectrum of the reaction mixture by subtraction of absorptions by the remaining reactants and by the products arising from CH_3ONO photooxidation (NO_2, HNO_3, HONO, HCHO, HCOOH, and CH_3ONO_2). In the case of isopropyl acetate, Figure 2 shows the presence of acetic anhydride as the major

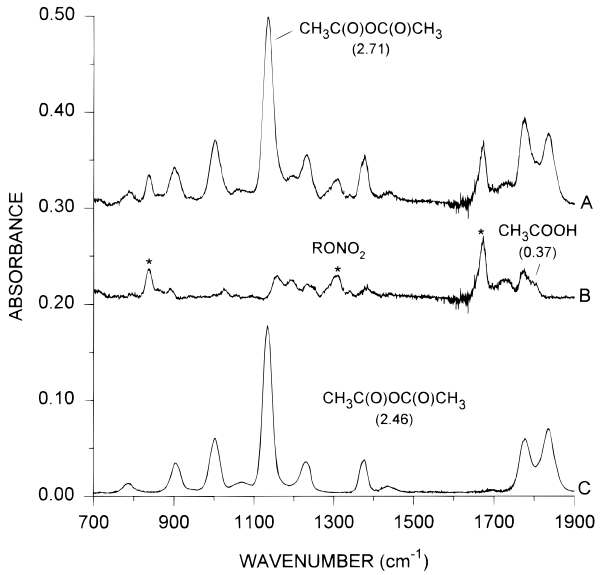

Figure 2. Infrared spectra from a $CH_3ONO-NO-$isopropyl acetate−air irradiation. (A) Products attributed to reaction of isopropyl acetate; photolysis time = 38 min; isopropyl acetate reacted = 3.62×10^{13} molecule cm^{-3}. (B) From (A) after subtraction of acetic anhydride absorptions. Asterisks denote $RONO_2$-type bands. (C) Reference spectrum of acetic anhydride. The numbers in parentheses are concentrations in units of 10^{13} molecule cm^{-3}.

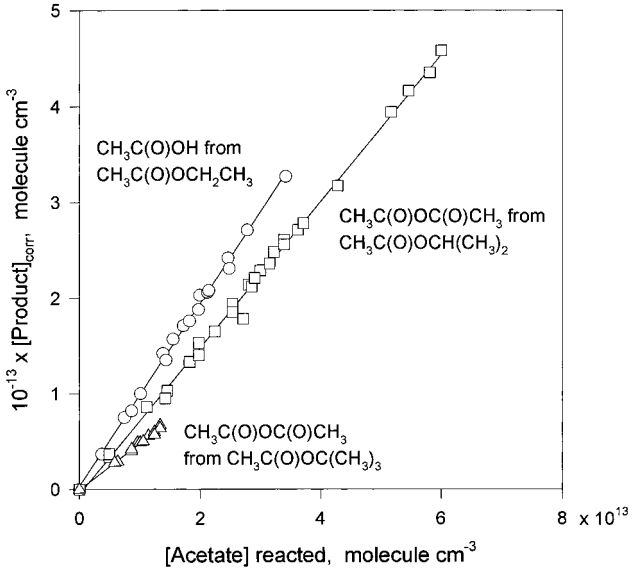

Figure 3. Plots of the amounts of acetic acid formed from ethyl acetate (corrected for secondary reactions; see text) and of acetic anhydride formed from isopropyl acetate and *tert*-butyl acetate against the amounts of the acetate reacted.

TABLE 1: Products Formed and Their Formation Yields from the Reactions of the OH Radical with Ethyl Acetate, Isopropyl Acetate, and *tert*-Butyl Acetate at 298 ± 2 K and Atmospheric Pressure of Air

acetate yield[a]	product	formation yield[a]
ethyl acetate	$CH_3C(O)OH$	0.96 ± 0.08
	$CH_3C(O)OC(O)CH_3$	<0.05
isopropyl acetate	$CH_3C(O)OH$	0.09 ± 0.03
	$CH_3C(O)OC(O)CH_3$	0.76 ± 0.07
	$CH_3C(O)CH_3$	0.24 ± 0.02
	CH_3CHO	<0.01
tert-butyl acetate	$CH_3C(O)OH$	<0.07
	$CH_3C(O)OC(O)CH_3$	0.49 ± 0.05
	$CH_3C(O)CH_3$	0.20 ± 0.02
	CH_3CHO	<0.01

[a] Indicated errors are two standard deviations combined with the estimated uncertainties in the acetate IR absorption band calibrations and the product IR absorption band or GC−FID response factor calibrations of ±5% each. The measured product concentrations have been corrected to take into account secondary reactions with the OH radical (see text).

product and acetic acid as a minor product. Consistent with the low rate constant for the reaction of the OH radical with *tert*-butyl acetate,[10,11] only low conversions (<7%) were obtained for *tert*-butyl acetate with irradiation of up to 65 min duration, and only acetic anhydride could be positively detected from the weak absorptions observed in the product spectra.

For all three acetates, the residual product spectra, such as those presented in Figures 1B and 2B, show the presence of $RONO_2$-type bands at ∼835, ∼1310, and ∼1670 cm^{-1}, and these appear most visible in Figure 2B due to the relatively high conversion of isopropyl acetate. The yield of the $RONO_2$ product(s) from isopropyl acetate is estimated[12] to be <4%. The $RONO_2$ band intensities relative to those of the major products (acetic acid and acetic anhydride) identified for each acetate decreased in the order *tert*-butyl acetate > isopropyl acetate > ethyl acetate.

For selected experiments involving isopropyl acetate and *tert*-butyl acetate, analyses for acetone and acetaldehyde were also carried out by GC−FID. The products observed and quantified from the FT-IR and GC−FID analyses were acetic acid from ethyl acetate; acetic acid, acetic anhydride, and acetone from isopropyl acetate; and acetic anhydride and acetone from *tert*-butyl acetate. Secondary reactions of the products were taken into account as described previously,[13] using literature OH radical reaction rate constants for the products and reactants (in units of 10^{-12} cm^3 $molecule^{-1}$ s^{-1}) of ethyl acetate, 1.67×10^{-12};[14] isopropyl acetate, 3.77×10^{-12};[11] *tert*-butyl acetate, 5.6×10^{-13};[11] acetic acid, 8×10^{-13};[1] acetic anhydride, 8.4×10^{-14} (estimated);[15,16] acetone, 2.19×10^{-13};[1] and acetaldehyde, 1.58×10^{-11}.[1] The multiplicative correction factors F to take into account secondary reactions increase with the rate constant ratio k(OH + product)/k(OH + ester) and with the extent of reaction,[13] and the maximum multiplicative factors F were 1.005 for acetic anhydride, 1.02 for acetone, 1.05 for acetic acid, and 2.20 for the potential formation of acetaldehyde from *tert*-butyl acetate. Figure 3 shows plots of the amounts of acetic acid formed from ethyl acetate and of acetic anhydride from isopropyl acetate and *tert*-butyl acetate plotted against the amounts of the acetates reacted (this figure also shows the small amount of *tert*-butyl acetate reacted compared to the experiments with ethyl acetate and isopropyl acetate). The products observed and their molar formation yields obtained by least-squares analyses of data such as those shown in Figure 3 are given in Table 1.

Discussion

Schemes 2A−4B show the expected[1−3] reaction mechanisms and potential products formed from the major alkoxy radicals generated after the initial OH radical reactions with ethyl acetate (Schemes 2A and 2B), isopropyl acetate (Schemes 3A and 3B), and *tert*-butyl acetate (Schemes 4A and 4B). The reactions leading to the alkoxy radicals are analogous to those shown in reactions 1, 2, and 3a. Reactions after H-atom abstraction from the $CH_3C(O)-$ groups of ethyl acetate and isopropyl acetate are not considered because these particular H-atom abstraction pathways are calculated to account for only ∼2.5% and ∼1.2% of the overall OH radical reaction, respectively.[15,16] Schemes 2A−4B are the basis for the following discussion.

SCHEME 2

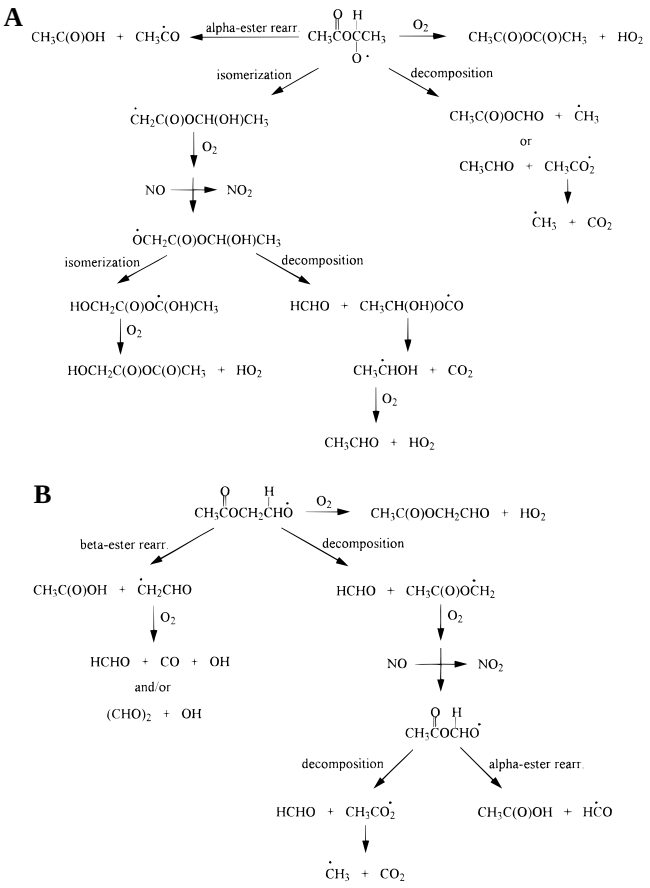

Ethyl Acetate. As illustrated in Figure 1, infrared analyses of irradiated $CH_3ONO-NO-$ethyl acetate$-$air mixtures showed the formation of acetic acid, and the molar formation yield of acetic acid as obtained from least-squares analysis of the data shown in Figure 3 is 0.96 ± 0.08. The FT-IR analyses showed no evidence for the formation of acetic anhydride, with an upper limit yield of <0.05. Experiments in which acetic anhydride was introduced into the chamber and its concentration monitored by FT-IR spectroscopy over a period of 2.5 h showed that acetic anhydride was stable under the experimental conditions employed and that no homogeneous or heterogeneous hydrolysis to acetic acid occurred on the time scales of the $CH_3ONO-NO-$ethyl acetate$-$air irradiations.

H-atom abstraction from the $-CH_2-$ and $-CH_3$ groups, leading to the alkoxy radicals shown in Schemes 2A and 2B, respectively, are estimated to account for 87% and 10%, respectively, of the overall OH radical reaction.[15,16] Scheme 2A shows that the only route to formation of acetic acid in significant yield is through the pathway labeled "alpha-ester rearr.", in which the alkoxy radical $CH_3C(O)OCH(\dot{O})CH_3$ undergoes a novel rearrangement through a five-membered transition state [α-ester rearrangement] shown in Scheme 5, which may or may not be a concerted reaction.

The overall reaction

$$CH_3C(O)OCH(\dot{O})CH_3 \rightarrow CH_3C(O)OH + CH_3\dot{C}O \quad (5)$$

is calculated[17,18] to be exothermic by ~5 kcal mol^{-1}, and the potential intermediate radical $CH_3\dot{C}(OH)OC(O)CH_3$ is calculated to be more stable than the $CH_3C(O)OCH(\dot{O})CH_3$ radical by the difference in the O$-$H and C$-$H bond dissociation energies of ~10$-$15 kcal mol^{-1}.[19] However, the presumed five-membered transition state is expected to have a significant ring strain of ~6 kcal mol^{-1},[20] and it is not clear whether the reaction proceeds via the intermediary of the $R\dot{C}(OH)OC(O)\acute{R}$ radical or as a concerted process.

SCHEME 3

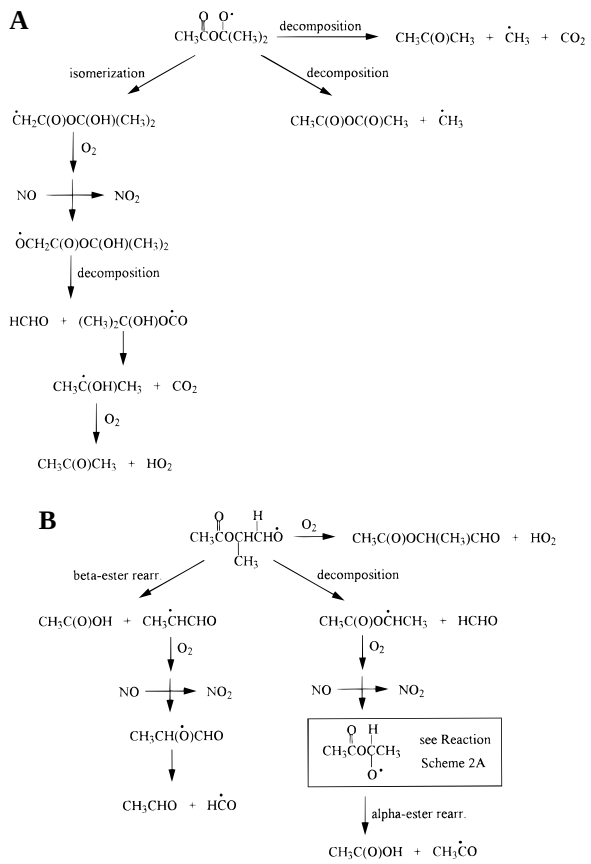

SCHEME 4

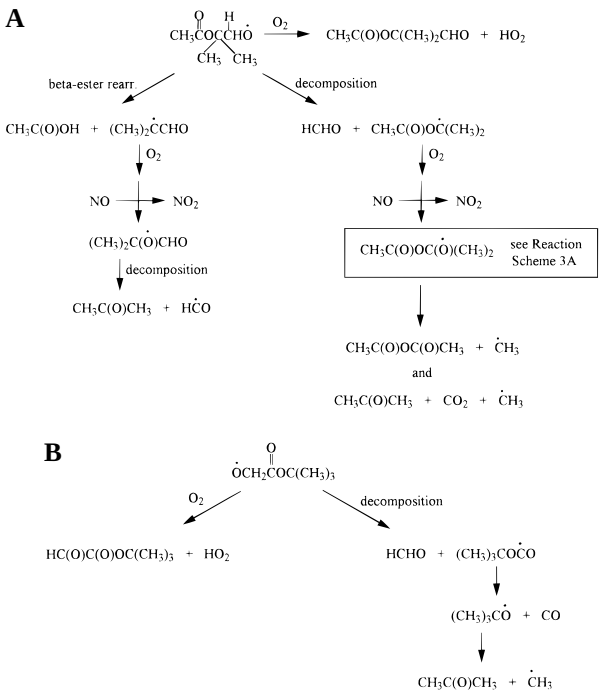

Although our acetic acid formation yield is unity within the experimental uncertainties, it is possible that the $CH_3C(O)OCH_2$-

SCHEME 5

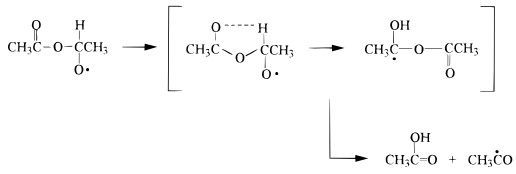

$CH_2\dot{O}$ radical formed after the minor H-atom abstraction reaction,

$$OH + CH_3C(O)OCH_2CH_3 \rightarrow H_2O + CH_3C(O)OCH_2\dot{C}H_2 \quad (9)$$

followed by reactions analogous to reactions 2 and 3a, reacts to form products other than acetic acid (Scheme 2B). Our data also do not rule out the $CH_3C(O)OCH(\dot{O})CH_3$ radical undergoing decomposition or reaction with O_2 to a minor extent (Scheme 2A). Clearly, at room temperature and atmospheric pressure of air, the major reaction of the $CH_3C(O)OCH(\dot{O})CH_3$ radical is via the novel α-ester rearrangement involving isomerization through a five-membered transition state, as shown in Scheme 5.

Isopropyl Acetate. As illustrated in Figure 2, infrared analyses of irradiated $CH_3ONO-NO-$isopropyl acetate−air mixtures showed the formation of both acetic anhydride and acetic acid. GC−FID analyses showed that acetone was also a reaction product, but that acetaldehyde was not formed in detectable amounts. The formation yields of acetic acid, acetic anhydride and acetone are given in Table 1, together with an upper limit to the formation yield of acetaldehyde derived from the GC−FID analyses (and taking into account secondary reactions of acetaldehyde).

H-atom abstraction from the >CH− and $-CH_3$ groups, leading to the alkoxy radicals shown in Schemes 3A and 3B, respectively, are estimated to account for 89% and 10%, respectively, of the overall OH radical reaction.[15,16] Reference to Schemes 3A and 3B show that the $CH_3C(O)OC(\dot{O})(CH_3)_2$ radical (the expected major initially formed alkoxy radical) must decompose by methyl elimination via C−C bond scission and, to a lesser extent, by decomposition via C−O bond scission and/or by 1,5-H shift isomerization through a six-membered transition state. This latter 1,5-H shift isomerization through a six-membered transition state is the "normal" isomerization pathway observed in alkoxy radicals formed from alkanes.[2,3] Because $CH_3C(O)CH_3$ is formed from decomposition via C−O bond scission and possibly after the 1,5-H shift isomerization (Scheme 3A), we cannot distinguish between these two reaction pathways. The analogous elimination of a methyl radical has been observed from the alkoxy radical $(CH_3)_2CHOC(\dot{O})(CH_3)_2$ formed after H-atom abstraction by the OH radical from the tertiary C−H bonds in diisopropyl ether.[21]

Decomposition of the $CH_3C(O)OCH(CH_3)CH_2\dot{O}$ radical formed after the minor H-atom abstraction channel leads to the $CH_3C(O)O\dot{C}HCH_3$ radical. Because this radical is the same radical as that formed after the dominant initial H-atom abstraction pathway from ethyl acetate (see Scheme 2A), acetic acid is the expected, as well as the observed, product. Comparison of our acetic acid yield of 9 ± 3% with the estimated percentage of reaction proceeding by H-atom abstraction from the two $-CH_3$ groups on the $-CH(CH_3)_2$ moiety (10%) suggests that decomposition of the $CH_3C(O)OCH(CH_3)CH_2\dot{O}$ radical dominates over the other potential reaction pathways (Scheme 3B). This conclusion is reinforced by GC−FID analyses, which showed that any formation of acetaldehyde (after taking into account reaction of acetaldehyde with the OH radical) had a molar yield of <0.01. It is estimated that the $CH_3CH(\dot{O})CHO$ radical will dominantly decompose at room temperature and atmospheric pressure of air.[1] Therefore, our lack of observation of CH_3CHO (with a formation yield of <0.01) suggests that the potential β-ester rearrangement proceeding by a six-membered transition state (Scheme 6) is not competitive with decomposition (Scheme 3B). The products observed and quantified account for 109 ± 8% of the isopropyl acetate reacted.

SCHEME 6

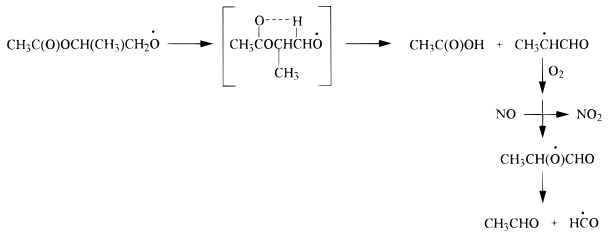

***tert*-Butyl Acetate.** H-atom abstraction from the $-CH_3$ groups of the $-C(CH_3)_3$ and $CH_3C(O)-$ moieties, leading to the alkoxy radicals shown in Schemes 4A and 4B, respectively, are estimated to account for 92% and 8%, respectively, of the overall OH radical reaction.[15,16] As shown in Scheme 4A, H-atom abstraction from the $-C(CH_3)_3$ group can lead, after decomposition of the $CH_3C(O)OC(CH_3)_2CH_2\dot{O}$ radical, to HCHO plus the $CH_3C(O)O\dot{C}(CH_3)_2$ radical, with the latter radical being identical to that formed after H-atom abstraction from the >CH− group in isopropyl acetate. Therefore, based on our product data for the isopropyl acetate reaction, decomposition of the $CH_3C(O)OC(CH_3)_2CH_2\dot{O}$ radical should lead to acetic anhydride and acetone with an acetone/acetic anhydride yield ratio of 0.32 ± 0.04.

Acetone plus acetic acid could be formed by a β-ester rearrangement involving a six-membered transition state; however, acetic acid was not observed from the *tert*-butyl acetate reaction (with an upper limit yield of 0.07) and, as discussed above, the analogous process was not observed in the isopropyl acetate reaction. It should be noted, however, that due to the low conversion of *tert*-butyl acetate the nondetection by FT-IR analyses of acetic acid from the dominant alkoxy radical formed from *tert*-butyl acetate (Scheme 4A) is not conclusive evidence against the occurrence of the β-ester rearrangement. Decomposition of the $(CH_3)_2C(\dot{O})CHO$ radical to $CH_3C(O)CH_3 + H\dot{C}O$ is calculated to be almost thermoneutral and 12.5 kcal mol^{-1} more favorable than the endothermic decomposition to $CH_3C(O)CHO + \dot{C}H_3$,[17,18] and hence acetone would be the expected coproduct to acetic acid in the β-ester rearrangement.

Acetone (plus HCHO coproduct) can also be generated by decomposition of the $\dot{O}CH_2C(O)OC(CH_3)_3$ radical formed after H-atom abstraction from the $CH_3C(O)-$ group, the predicted minor H-atom abstraction channel (Scheme 4B). Our acetic anhydride and acetone formation yields are consistent with decomposition of the $\dot{O}CH_2C(O)OC(CH_3)_3$ radical (~4 ± 4%) and decomposition of the $CH_3C(O)OC(CH_3)_2CH_2\dot{O}$ radical (65 ± 6%). The remaining 31 ± 8% of the reaction pathways not accounted for must then involve reactions of the $CH_3C(O)OC(CH_3)_2CH_2\dot{O}$ and $\dot{O}CH_2C(O)OC(CH_3)_3$ radicals with O_2 leading to unobserved products and/or measurement uncertainties due to the small amounts of *tert*-butyl acetate reacted.

Conclusions

Our product studies of the OH radical-initiated reactions of ethyl acetate, isopropyl acetate and *tert*-butyl acetate in the presence of NO show that alkoxy radicals of structure $CH_3C(O)OCH(\dot{O})R$ undergo a novel α-ester rearrangement reaction involving migration of the H-atom on the alkoxy carbon to the oxygen atom in the C═O group through a five-member transition state (Scheme 5), resulting in the formation of acetic acid plus the acyl ($R\dot{C}O$) radical. In contrast, the analogous *β*-ester rearrangement involving a six-member transition state (Scheme 6) was not observed in the reaction systems studied here. However, in the ethyl acetate and isopropyl acetate reactions the alkoxy radicals which could potentially undergo the *β*-ester rearrangment are predicted to be formed in only low yield (≤10%) and there are other competing reaction pathways, and for the $CH_3C(O)OC(CH_3)_2CH_2\dot{O}$ radical formed from *tert*-butyl acetate the competing decomposition is expected to be rapid.

The α-ester rearrangement pathway accounts for the observation of Stemmler et al.[22] of acetic acid from the reactions of the OH radical with 2-hydroxy-2-methylpropyl acetate [$CH_3C(O)OCH_2C(OH)(CH_3)_2$] and, to a lesser extent, isobutyl acetate [$CH_3C(O)OCH_2CH(CH_3)_2$]. This new alkoxy radical reaction pathway must be incorporated into chemical mechanisms for the tropospheric degradation reactions of esters.

While it is also possible that a similar reaction pathway occurs in carbonyl compounds for alkoxy radicals of the structure,

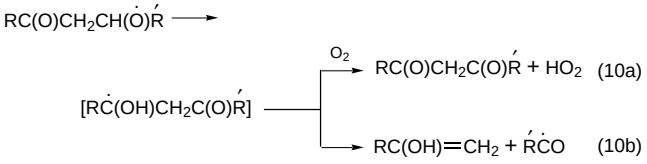

reaction channel (10a) leads to the same products as are formed by reaction of the alkoxy radical with O_2. As yet no evidence for or against this rearrangement reaction [10a and/or 10b] in carbonyls exists. However, for the $CH_3C(O)CH_2CH(\dot{O})CH_3$ radical the overall reaction 10b is calculated to be endothermic by 5−6 kcal mol^{-1}.[17,18]

Acknowledgment. The authors gratefully thank the U.S. Environmental Protection Agency, Office of Research and Development (Assistance Agreement R-825252-01-0) for supporting this research. While this research has been supported by the U.S. Environmental Protection Agency, it has not been subjected to Agency review and, therefore, does not necessarily reflect the views of the Agency, and no official endorsement should be inferred.

References and Notes

(1) Atkinson, R. *J. Phys. Chem. Ref. Data, Monogr.* **1994**, *2*, 1.
(2) Atkinson, R. *J. Phys. Chem. Ref. Data* **1997**, *26*, 215.
(3) Atkinson, R. *Int. J. Chem. Kinet.* **1997**, *29*, 99.
(4) Atkinson, R.; Carter, W. P. L. *J. Atmos. Chem.* **1991**, *13*, 195.
(5) Carter, W. P. L. 1997. Unpublished data.
(6) Atkinson, R.; Carter, W. P. L.; Winer, A. M.; Pitts, J. N., Jr. *J. Air Pollut. Control Assoc.* **1981**, *31*, 1090.
(7) Tuazon, E. C.; Atkinson, R. *Int. J. Chem. Kinet.* **1989**, *21*, 1141.
(8) Atkinson, R.; Aschmann, S. M. *Environ. Sci. Technol.* **1995**, *29*, 528.
(9) Taylor, W. D.; Allston, T. D.; Moscato, M. J.; Fazekas, G. B.; Kozlowski, R.; Takacs, G. A. *Int. J. Chem. Kinet.* **1980**, *12*, 231.
(10) Smith, D. F.; Kleindienst, T. E.; Hudgens, E. E.; McIver, C. D.; Bufalini, J. J. *Int. J. Chem. Kinet.* **1992**, *24*, 199.
(11) Le Calvé, S.; Le Bras, G.; Mellouki, A. *Int. J. Chem. Kinet.* **1997**, *29*, 683.
(12) Tuazon, E. C.; Atkinson, R. *Int. J. Chem. Kinet.* **1990**, *22*, 1221.
(13) Atkinson, R.; Aschmann, S. M.; Carter, W. P. L.; Winer, A. M.; Pitts, J. N., Jr. *J. Phys. Chem.* **1982**, *86*, 4563.
(14) El Boudali, A.; Le Calvé, S.; Le Bras, G.; Mellouki, A. *J. Phys. Chem.* **1996**, *100*, 12364.
(15) Kwok, E. S. C.; Atkinson, R. *Atmos. Environ.* **1995**, *29*, 1685.
(16) Kwok, E. S. C.; Aschmann, S. M.; Atkinson, R. *Environ. Sci. Technol.* **1996**, *30*, 329.
(17) Stein, S. E. National Institute of Standards and Technology Database 25; Structures and Properties Database and Estimation Program, Version 2.0; Chemical Kinetics and Thermodynamics Division, NIST; Gaithersburg, Maryland, 1994.
(18) Atkinson, R.; Baulch, D. L.; Cox, R. A.; Hampson, R. F., Jr.; Kerr, J. A.; Rossi, M. J.; Troe, J. *J. Phys. Chem. Ref. Data* **1997**, *26*, 1329.
(19) Kerr, J. A. Strengths of Chemical Bonds. In *Handbook of Chemistry and Physics*, 74th ed.; Lide, D. R., Ed.; CRC Press: Boca Raton, FL, 1993−1994; pp 9-123−9-145.
(20) Benson, S. W. *Thermochemical Kinetics*, 2nd ed.; Wiley: New York, 1976.
(21) Wallington, T. J.; Andino, J. M.; Potts, A. R.; Rudy, S. J.; Siegl, W. O.; Zhang, Z.; Kurylo, M. J.; Huie, R. E. *Environ. Sci. Technol.* **1993**, *27*, 98.
(22) Stemmler, K.; Mengon, W.; Kerr, J. A. *J. Chem. Soc., Faraday Trans.* **1997**, *93*, 2865.